A Framework for Estimating Bone Strength Along the Distal Radius and the Effect of Eccentric Axial Load Position

+Wagner, D W; Lindsey, D P; Beaupre, G S
Bone & Joint Center of Excellence, VA Palo Alto Health Care System, Palo Alto, CA 94304
dwwagner@va51.stanford.edu

INTRODUCTION:

Tissue level finite element (FE) models derived from microCT scans have demonstrated the potential for estimating macroscopic bone strength of the distal radius with a reasonable degree of fidelity [1,2]. However, the computational requirements, documented benefit over traditional measures, and ability to validate those models with experimental data have limited the widespread adoption of those models in the clinical environment. Due to those limitations, microFE models of the distal radius are often only evaluated in constrained compression, resulting in a single representative value of bone strength [3,4,5]. However, Troy and Grabiner [6] showed that the loading condition (i.e. combination of axial compression and bending) significantly affects the predicted failure force, suggesting that a single bone strength value is not appropriate for all conditions. The purpose of this study is to present a framework for analyzing microCT axial images of the distal radius using an engineering based approach for estimating fracture strength from axial and bending forces that is not constrained by extensive computational requirements (i.e. experience with microFE software, analysis times exceeding several hours, substantial computer RAM, etc.). The effect of the position of the axial slice and the position of the eccentric axial force are also presented.

METHODS:

Five left radii were excised from fresh frozen cadavers and analyzed as described below. The results for a single specimen, which were typical of all the analyzed specimens, are presented. The results of the excised left radius presented here were from a forearm harvested from a 74 year-old male donor (178 cm, 69 kg). The intact radius was scanned with a Scanco vivaCT 40 microCT scanner using the following settings: 55kVp, 145 μA, 1000 ms integration time, 19 μm voxel size; a 1200 mg-HA/cm^3 beam hardening correction algorithm was also applied. Ten evenly spaced slices along the axial direction (Figure 1, lower right) were used for the analysis. Bone tissue was segmented using a constant threshold and a peeling procedure of two voxels was applied to reduce partial volume effects [7]. A custom procedure, similar to that used by Renders et al. [8], was used to assign voxel-based elastic moduli to each pixel. For each slice, the elastic modulus weighted centroid (x^*, y^*), flexural rigidity (I^*_{xx} and I^*_{yy}), generalized product of inertia (I^*_{xy}), and axial stiffness A^* were calculated. For an input eccentric load position defined at ($\hat{x}$, $\hat{y}$), the generalized flexural formula (Eq. 1) was used to calculate the strain at each point (x,y) due to a load of magnitude *P* [9].

$$\varepsilon_{zz}(x,y) = \frac{P}{A^*} + \frac{P\left((\hat{y}-y^*)I^*_{yy}-(\hat{x}-x^*)I^*_{xy}\right)}{I^*_{yy}I^*_{xx}-(I^*_{xy})^2}(y-y^*) + \frac{P\left((\hat{x}-x^*)I^*_{xx}-(\hat{y}-y^*)I^*_{xy}\right)}{I^*_{yy}I^*_{xx}-(I^*_{xy})^2}(x-x^*) \quad \text{Eq. 1}$$

For each slice, a macroscopic failure criterion was applied such that a fracture failure was defined to occur when 2% [2] of the bone tissue voxels exceeded the yield strain criteria for compression, tension, or a combination of the two. Bone tissue yield strains of 0.85% in compression and 0.61% in tension [10] were used. Ten evenly spaced eccentric load positions between Lister's Tubercle and an analogous point on the volar surface were evaluated (Figure 1) and the necessary compressive force individually applied at each of those locations to produce macroscopic failure was calculated.

RESULTS:

For each axial slice, the smallest predicted failure force occurred when the eccentric load was applied along the dorsal aspect of the radius and the next smallest when the load was applied along the volar aspect (Figure 1). In Figure 1, the 10 red dots depicted in the axial image (upper left) indicate the locations of the eccentric axial forces for 10 unique load cases. For a given axial slice (lower right), the 10 color-coded boxes in the corresponding column of the failure force plot (upper right) indicate the failure loads for that slice for the 10 unique eccentric axial force locations. On average, the predicted compressive failure force increased in magnitude as the analyzed axial slice moved proximally. For the most dorsal force position, the predicted failure force ranged from -1250 to -1897, a 52% increase in magnitude. For the eccentric load near the midline of the cross section (the 6th most dorsal load in Figure 1) the predicted failure force ranged from -1644 to -6960 proceeding from distal to proximal, a 320% increase in magnitude. In contrast, the failure load associated with pure axial compression ranged from -8384 N (2nd most distal slice) to -11310 N (most proximal slice), a 35% increase in magnitude.

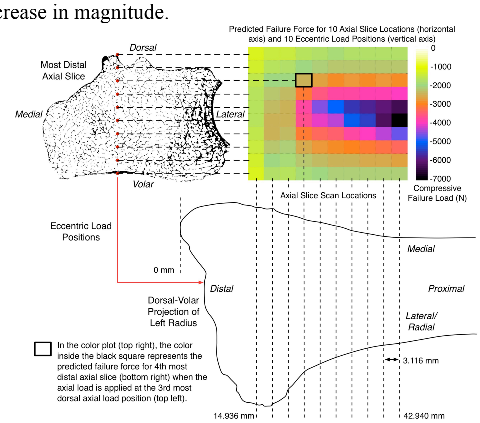

***Figure 1**. Predicted failure force for ten eccentric axial load positions and ten axial slice locations.*

DISCUSSION:

A new framework for evaluating distal radius strength using the generalized flexural formula was proposed. The limited computational overhead associated with the proposed framework is potentially its greatest strength, allowing for multiple axial slices and loading conditions to be evaluated within a few seconds. Additionally, the output metric of force (Newtons) is similar to the tissue-level FE models allowing for direct comparison across failure modes and potentially less ambiguity than other metrics (i.e. flexural rigidity or axial stiffness). Several aspects of the framework must be evaluated in greater detail prior to justification that the derived metrics would provide additional clinically relevant information over traditional measures. First, the definition of macroscopic failure (i.e. fracture) as implemented here is dependent on the assumed yield strain of bone tissue and the total number of tissue elements that must 'fail' prior to macroscopic fracture. Pistoia et al. [2] conducted a sensitivity study using a similar failure criterion applied to a 3D FE model and found that predictions best fit the experimental data when 2% of the model voxels exceeded the yield strain, however that approach may not be the most robust when only using 2D axial slices. Second, to predict clinically relevant fracture risk, appropriate boundary conditions must be derived and validated ex-vivo, a procedure that has yet to be performed under any modeling paradigm. Third, the 3D structure is analyzed here as a simplified 2D slice (or group of slices) and the effect of that simplification on the fidelity of predicted fracture force previously observed for 3D FE models must be evaluated. The results from the color figure highlight that for axial loads with high eccentricity, either dorsal or volar, the strength increases only moderately when proceeding from distal to proximal slices. For axial loads applied more centrally, the distal slices are substantially weaker than the proximal slices. Future tools, particularly those proposed to enhance the clinical assessment of bone strength, must identify appropriate input loading conditions so that an accurate relationship between relevant failure modes can be derived.

SIGNIFICANCE:

A new framework for predicting bone strength using engineering based methods that is not dependent on computationally intensive processes, a significant impediment in applying such models in the clinical arena, is proposed.

REFERENCES:

[1] Macneil et al., Bone, 42:1203-13, 2008; [2] Pistoia et al., Bone, 30:842-48, 2002; [3] Boutroy et al., J Bone Miner Res, 23:392-99, 2007; [4] Dalzell et al. Osteoporos Int, 20:1683-94, 2009; [5] Melton et al. J Bone Miner Res, 22:1442-8, 2007; [6] Troy et al., J Biomech, 40:1670-5, 2007; [7] Fajardo et al., Bone, 44:176-184, 2009; [8] Renders et al., J Biomech, 44:402-7, 2011; [9] Carpenter et al., J Bone Miner Res., 20:1533-42, 2005; [10] Morgan et al., J Biomech, 34:569-77, 2001.

ACKNOWLEDGEMENTS:

Supported by the Dept of Veterans Affairs, Rehab R&D (Proj. A6816R).